Vol. 685: 1–18, 2022
https://doi.org/10.3354/meps13982

MARINE ECOLOGY PROGRESS SERIES
Mar Ecol Prog Ser

Published March 10

FEATURE ARTICLE

Entrainment and development of larval fish assemblages in two contrasting cold core eddies of the East Australian Current system

Valquiria Garcia[1,2], Hayden T. Schilling[1,3], Derrick O. Cruz[1], Steven M. Hawes[4], Jason D. Everett[1,3,5], Moninya Roughan[6], Anthony G. Miskiewicz[1,7], Evgeny A. Pakhomov[8,9], Andrew Jeffs[10], Iain M. Suthers[1,3,*]

[1]School of Biological, Earth & Environmental Sciences, University of New South Wales, Sydney, NSW 2052, Australia

Full author addresses are given in the Appendix

ABSTRACT: Cyclonic eddies are diverse in their size, age, upwelling and behaviour, which has significant implications for fisheries production and connectivity when they interact with the continental shelf. To ascertain coastal entrainment by eddies, we compared the larval fish community of 2 contrasting cyclonic eddies in 3 depth strata (0–5, 5–50, 50–100 m), and with the adjacent shelf community. The frontal cyclonic eddy was smaller and younger than the mesoscale cyclonic eddy. A larval fish entrainment index, based on the ratio of coastal to oceanic taxa, revealed the relative abundance of coastal larvae entrained into the upper mixed layer of the frontal eddy, consistent with published numerical modelling studies of similar eddies. The frontal eddy had a high abundance of commercially important coastal taxa entrained from the inner shelf. However, the adjacent inner shelf water and putative location for frontal eddy formation had recently been displaced by the East Australian Current, resulting in the larval fish community being dominated by oceanic taxa. The spatial and temporal dynamics of coastal entrainment into the larger, older cyclonic eddy and the adjacent shelf region were revealed by mixtures of coastal and oceanic taxa in each of the depth strata. The larger cyclonic eddy had a higher biomass of zooplankton, indicating the cumulative effects of eddy age and production. Eddies which interact with the shelf enable cross-shelf mixing and may contribute to coastal fisheries.

KEY WORDS: Ichthyoplankton · Zooplankton · Cyclonic eddy · Tasman Sea · Connectivity · Cross-shelf exchange

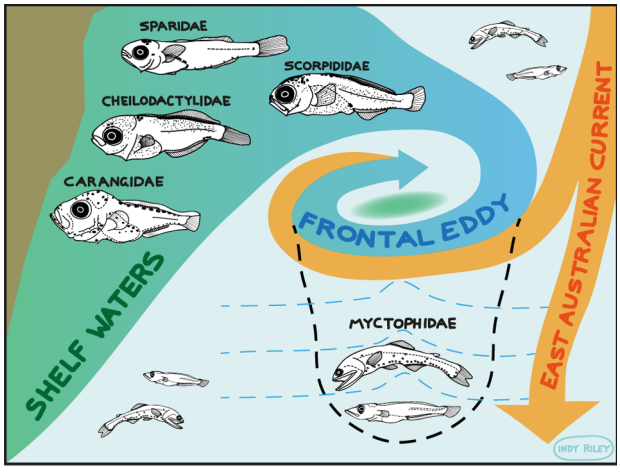

A mixture of coastal and oceanic fish larvae indicated how an eddy, forced by a boundary current, entrained coastal waters offshore

Graphic: Indiana Riley

1. INTRODUCTION

Eddies are important habitats for larval fish as they facilitate production and retention, which are both key steps in larval survival and population connectivity (Bakun 2006, Atwood et al. 2010, Govoni et al. 2013, Olivar et al. 2016, Shulzitski et al. 2016). In general, cyclonic eddies, termed 'cold-core' eddies, are upwelling favourable, drawing cool water and nutrients into the euphotic zone. As a result, cyclonic eddies may be (but are not always) characterised by higher chlorophyll *a* (chl *a*) concentrations compared

*Corresponding author: i.suthers@unsw.edu.au

Publisher: Inter-Research · www.int-res.com

to anticyclonic eddies (Everett et al. 2012). Cyclonic eddies are also associated with enhanced growth and survival of larval fish (Nakata et al. 2000, Logerwell & Smith 2001, Hardman-Mountford et al. 2003). For example, compared to anticyclonic eddies, cyclonic eddies may contain from 3- to 10-fold more larval fish (Muhling et al. 2007, Matis et al. 2014). Such eddies off Florida (USA) are an important staging ground for larval fish (Shulzitski et al. 2015), because fish associated with cyclonic eddies had growth characteristics similar to new recruits that survived and settled onto coral reefs (Sponaugle et al. 2005, Shulzitski et al. 2016). For some coasts, however, offshore transport may be detrimental to recruitment, such as for larval sardine in the California Current system (Nieto et al. 2014), and therefore region-specific work is necessary to examine the fate of larval fish entrained into eddies.

Smaller eddies, i.e. those <60 km in diameter, are increasingly recognised as important features of the seascape (Kasai et al. 2002, Govoni et al. 2013, Mullaney & Suthers 2013). Such frontal eddies form as instabilities or cyclonic meanders at the frontal edge of western boundary currents (Lee et al. 1991) and are often referred to as billows or spin-off eddies. Off the east coast of Australia, a 12 mo synthesis of coastal high-frequency radar observations showed that frontal eddies form irregularly but on average every week (Schaeffer et al. 2017). Their biological configuration may include entrainment of plankton from the inner shelf (Everett et al. 2015) and development of the entrained assemblages over time. If they are close to the coast, frontal eddies can therefore serve as habitat for coastal larvae and contribute to the connectivity and recruitment to coastal populations (Booth et al. 2007, Mullaney et al. 2014, Malan et al. 2020). Cyclonic eddies seem especially capable of entraining coastal water and the associated larvae, providing they have interacted with the shelf or slope (Nakata et al. 2000, Holliday et al. 2011). When they interact with the shelf, frontal eddies may entrain shelf water from over 4 degrees of latitude during several days, increasing in size by a factor of 5 (Everett et al. 2015), with uplifting velocities of 10s of metres per day (Lee et al. 1991, Schaeffer et al. 2017). Everett et al. (2015) estimated that over 95% of the volume of a frontal eddy was derived from shelf water, entraining ~0.5 Sv d^{-1}. In their study, a numerical model revealed that most of the entrained water was in the upper mixed layer (<50 m depth), driven by the relative densities of the shelf and eddy waters.

Studies of the vertical distribution of fish larvae in eddies have generally shown highest abundances in the upper depth intervals, with decreasing abundances with increasing depth layers (Muhling et al. 2007, Moyano et al. 2014, Shulzitski et al. 2018, Hawes et al. 2020). Other factors that can affect larval vertical distributions are diel vertical migrations (Muhling et al. 2007, Moyano et al. 2014) and ontogenetic changes in depth distributions (Shulzitski et al. 2018, Hawes et al. 2020). Gray & Miskiewicz (2000) reported on patterns of vertical distribution of larval fish assemblages in coastal waters of southeastern Australia. They found that assemblages were depth stratified between the surface and midwater depths of 20–30 m during the day in all seasons, with higher abundances and diversity in the midwater strata. Unfortunately, data on the depth distribution of larval fish assemblages in East Australian Current (EAC)-derived eddies are lacking, and most studies in the southeast Australian region have assumed that higher larval abundances occur in the upper mixed layer (e.g. Syahailatua et al. 2011, Matis et al. 2014). Matis et al. (2014) observed the entrainment of coastal larval fish into the surface waters of a large cyclonic eddy that had recently shifted landward from the Tasman Sea and interacted with the shelf. In contrast, there was a paucity of coastal larvae in an adjacent anticyclonic eddy that flowed across the shelf and slope, and it was possible that the anticyclonic eddy may have entrained larvae at depth, or they were lost from the eddy by either mortality, or by growth and development. Eddy shape can also determine retention of particles such as larvae, where an increase in elongation leads to leakage of particles (Cetina-Heredia et al. 2019b).

Consequently, there is a diversity of eddy circulation, size and age, and biological processes (e.g. Moyano et al. 2014, Nieto et al. 2014, Olivar et al. 2016). Without detailed knowledge of the history of the eddy (e.g. Atwood et al. 2010, Everett et al. 2015), it is difficult to understand the biological processes and implications for continental shelf ecosystems. What is needed is an indicator of the initial coastal entrainment and temporal changes of the entrained larval fish assemblage in the frontal eddy through growth, mortality or metamorphosis, relative to the oceanic larval assemblage, often dominated by larvae of the diverse and abundant family of larval lantern fishes (Myctophidae).

In this study, we compared the larval fish assemblages of 2 contrasting cyclonic eddies of the East Australian Current system — a large mesoscale cyclonic eddy (>160 km diameter) and a nearby smaller frontal eddy (~35 km diameter). We also examined the zooplankton particle size structure between eddies to provide an ecological context to tracking water types

and plankton assemblages. The physical characteristics of these 2 eddies were described by Roughan et al. (2017), as part of a detailed account of locating and contrasting the physical characteristics of each eddy. The larger mesoscale cyclonic eddy was ~26 d old at the time of sampling and had briefly interacted with the shelf at latitude ~27° S, while the smaller frontal eddy was studied about a week after it formed on the shelf off the central New South Wales coast at latitude ~32° S. We expected the frontal eddy to entrain more inner shelf water and the associated coastal larval fish communities in a process detailed by Everett et al. (2015), compared to the larger mesoscale eddy which was typical for the region (Everett et al. 2012, Roughan et al. 2017). These 2 productive eddies, which are so ubiquitous in satellite imagery, presented an opportunity to compare the implications for their larval assemblages.

To investigate the interaction of eddies with the shelf, we propose a larval fish entrainment index, calculated as the ratio of abundances of coastal to oceanic taxa. The sum of coastally spawned taxa is a useful characteristic of shelf water (e.g. Schilling et al. 2022), while oceanic taxa are well represented by the diversity and abundance of larval Myctophidae (Mullaney et al. 2011). Such an approach could also include the zooplankton community as a biological property of the larval fish habitat (e.g. Suthers et al. 2006), as a practical way to compare the zooplankton among entrained and oceanic waters. The goal of this study was to compare the recently entrained larval fish assemblage in a young frontal eddy with an older and larger cyclonic eddy, and with the adjacent shelf water. During the voyage, the frontal eddy moved offshore and oceanic water was drawn onto the shelf, providing a useful test of the larval entrainment index. Specifically, we aimed to (1) determine the distribution of larvae in both cyclonic eddies in relation to the expected entraining process (Everett et al. 2015, Roughan et al. 2017); (2) examine the associated zooplankton size spectrum of the 2 eddies to provide insight into the biological processes; and (3) demonstrate the use of the larval fish entrainment index as a tool to understand the entrainment process.

2. MATERIALS AND METHODS

2.1. Study area

An 18 d research voyage was conducted during the austral early winter in June 2015, to investigate the coastal entrainment and development of the larval fish community associated with 2 cyclonic eddies in the EAC (described by Roughan et al. 2017). The large mesoscale cyclonic eddy was located at ~28.75° S, 154.5° E (Fig. 1A,B). It was 160 km in diameter and ~26 d old on the day of sampling (referred to as 'Murphy' by Roughan et al. 2017). The smaller and younger frontal eddy ('Freddy') was located at ~32.6° S, 153.2° E, had a 35 km diameter and ~7 d since formation (Fig. 1C). Two coastal regions (coast–south [Coast–S] and coast–north [Coast–N]) were also sampled on the shelf around the 100 m isobath to characterise the coastal assemblage (Fig. 1B,C). Near-real time satellite data and surface drifting buoys were used to physically characterise the eddy and sampling stations (see Roughan et al. 2017).

Briefly, the northern cyclonic eddy had a rotation rate of ~4 d and a Rossby number of 0.30; the southern frontal eddy had a rotation rate of 1.4 d and Rossby number ~0.6 at the surface (Roughan et al. 2017). Surface Velocity Program drifters drogued at 15 m showed that both eddies moved a straight-line distance of ~17 km d^{-1} southwards (cyclonic) or southeast (frontal; Roughan et al. 2017). In the cyclonic eddy, the 17°C isotherm was raised from 225 to 160 m over 75 km (0.6 m km^{-1}), whereas in the frontal eddy, the same isotherm was raised from 210 to 125 m in 25 km (3.5 m km^{-1}).

The vertical structure of both eddies was examined with a towed body (a 1.2 m wide MacArtney System Triaxus), which profiled temperature, conductivity, depth, chl *a* fluorescence, dissolved oxygen and transmissivity, from ~5 to >150 m depth at 8 knots (~4 m s^{-1}; Fig. 1B,C). The Triaxus system cannot sample shallower depths than 5 m due to technical limitations and likelihood of interference from bubbles in the surface layer. In the cyclonic eddy, the Triaxus was towed on 5 June for 10 h between 17:00 and 03:00 h local time. In the frontal eddy, the Triaxus was towed on 9 and 10 June for 5 h from the shelf into the eddy (from 16:54 to 21:44 h local time). Unfortunately, the Triaxus could not be deployed at the 2 coastal sites over the continental shelf (Fig. 1).

Mounted on the top of the Triaxus was a laser optical plankton counter (LOPC) (Herman et al. 2004), which counted and estimated size and biomass of zooplankton 0.2 up to 12 mm equivalent spherical diameter (ESD). Particles were binned into 32 logarithmically equal size intervals of 0.2 mg. Zooplankton biomass was calculated from the volume of a prolate spheroid (ratio of 1:3 width:length) and the specific gravity of water (Suthers et al. 2006), which was then converted to a normalised biomass by dividing the biomass of each size bin by the width of each

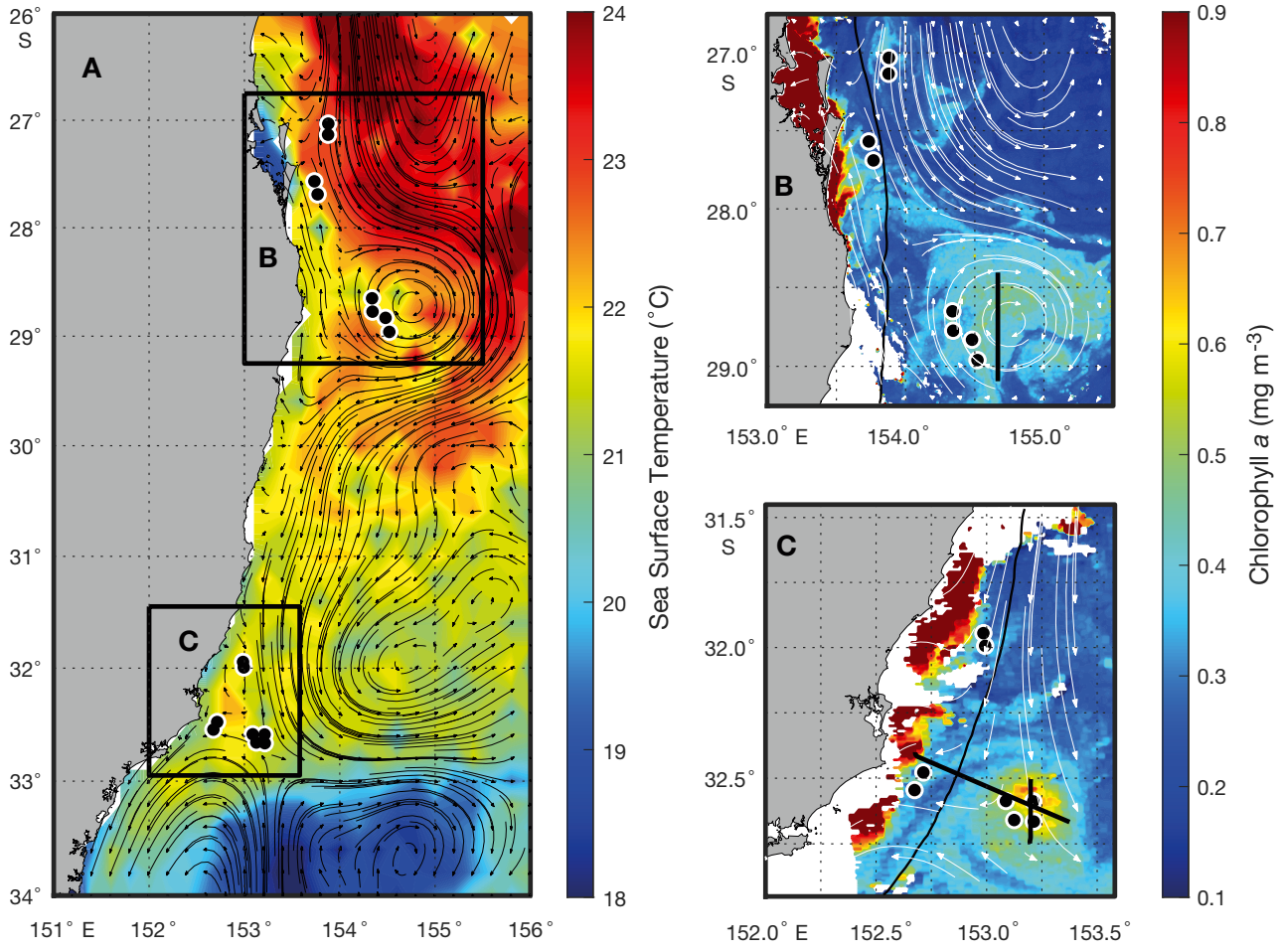

Fig. 1. Remotely sensed images off the east coast of Australia of (A) sea surface temperature (from MODIS-Aqua); ocean colour images with the sampling locations at (B) the northern cyclonic eddy and the 4 shelf stations north of the eddy (referred to as Coast–N) and (C) at the southern frontal eddy and the 4 shelf stations west of the eddy (referred to as Coast–S). Circles show the 4 sampling locations in each of the 4 regions (shelf, eddy, north and south). The solid black lines across both eddies in panels B and C show the Triaxus transects supporting the laser optical plankton counter (see Figs. S7–S9 in the Supplement)

bin. The use of a normalised biomass size spectrum (NBSS) enables inter-comparison of different studies that may use different size classes. We extracted the following 5 metrics of the NBSS (Krupica et al. 2012), for each eddy and depth approximating the positions and depths of the plankton samples (see Section 2.2): zooplankton abundance (ind. m^{-3}) and biomass (mg m^{-3}), the linear least-squares regression slope and intercept (NBSS slope, NBSS intercept m^{-3}), and geometric mean size (GMS, µm). The NBSS slope summarises the ratio of the zooplankton mortality to growth rate (Suthers et al. 2021), and the NBSS intercept represents the normalised zooplankton biomass at 1 mg wet weight (i.e. the intercept at 10^0 mg; Krupica et al. 2012). A flatter slope than −1 will have zooplankton growth greater than mortality, whereas a steeper slope than −1 will experience greater mortality than growth (Suthers et al. 2021).

2.2. Sampling procedures

Zooplankton and larval fish were sampled at night using a 1 m^2 surface net and a 1 m^2 multiple opening and closing net and environmental sensing system (MOCNESS) fitted with 500 µm mesh, with each net towed at 2–3 knots (1–1.5 m s^{-1}) for approximately 10 min and filtering ~750 m^3. The surface net sampled 1 depth stratum (0–1 m) and the MOCNESS sampled 2 depth strata (5–50 and 50–100 m) resulting in 3 depth strata (n = 2 per stratum) at the 4 locations or habitats (i.e. 2 eddies and 2 adjacent shelf areas). Each location had 2 replicate stations on different nights of the voyage nested within each location (Fig. 1). Therefore, the sampling design was 4 locations × 3 depth strata × 4 replicate stations (n = 2 tows per depth), totalling 96 samples. However, 3 samples were lost or incorrectly preserved resulting in a total of 93 sam-

ples (for further details see 'Voyage Summary' in Suthers 2015). A General Oceanics mechanical flowmeter attached to the nets allowed the calculation of volumes sampled, and depth, temperature and salinity were electronically recorded during each tow. To determine the corresponding water mass, we used the more precise data from vertical profiles of the vessel's calibrated conductivity-temperature-depth (CTD) cast to >500 m before or after each plankton tow (see Table 1 in Roughan et al. 2017 for CTD cast metadata). The CTD was a 24-bottle rosette supporting a SeaBird SBE32.

Samples were either sorted at sea or back in the laboratory. At sea, most fresh plankton was sorted on ice, and fish larvae were preserved in 95% ethanol and then transferred to 70% ethanol. The plankton samples were re-examined on land to ensure that all larvae were removed. Some samples were fixed immediately in seawater containing 5% formalin buffered with sodium carbonate to conserve the otoliths. On land, these formalin-fixed samples were sorted within 3 to 4 mo (as long-term storage in sodium carbonate solution can cause bleaching of the melanophores) and transferred to 70% ethanol. All fish larvae were identified to family using keys by Neira et al. (1998) and Leis & Carson-Ewart (2000), and densities were standardised to number of larvae 100 m^{-3}. To align with previous terminology, we refer to both density and abundance (e.g. Matis et al. 2014, Hinchliffe et al. 2021).

2.3. Statistical analysis

Analyses of larval abundance and diversity were conducted using model-based approaches, as these have significant advances over more traditional distance-based methods (Warton et al. 2012, Hui et al. 2015). Analysis was first conducted using univariate response variables and then with multivariate community composition. All analyses were conducted in R v3.4.3 (R Core Team 2017). All results are presented with exact p-values and use the traditional alpha of 0.05 to assess the significance of post-hoc tests.

Diversity was compared among eddies and depths using a 2-factor ANOVA with depth and location as fixed factors. Diversity was analysed using Shannon's index of diversity and was calculated using the 'diversity' function in the R package 'vegan' v2.5.2 (Oksanen et al. 2018). Within samples, Pielou's evenness index, which is another component of diversity, was highly correlated with Shannon's index of diversity ($R^2 = 0.83$) and therefore evenness was not considered further. Since the Myctophidae dominated larval abundance, we conducted separate analyses for myctophids and for the rest of the community ('other') with generalised linear models (GLMs) with a negative binomial distribution including location (4 locations: cyclonic eddy, frontal eddy, Coast–N, Coast–S) and depth (3 depths: 0–5, 5–50 and 50–100 m) as fixed factors and log(volume filtered) as an offset. A volume offset was used here due to the increasing number of larvae sampled with increasing volume. The overdispersion parameters for the GLMs were total abundance: 4.11, Myctophidae abundance: 3.25 and 'other' abundance: 4.12. Post-hoc tests for the univariate analyses were conducted using estimated marginal means calculated using the 'emmeans' function in the R package 'emmeans' v1.3.0 (Lenth 2018), which applies an adjusted p-value to account for multiple testing. All model assumptions were checked using a simulation approach implemented using the 'DHARMa' R package (Hartig 2020; Figs. S1–S4 at www.int-res.com/articles/suppl/m685p001_supp.pdf).

Overall multivariate community composition of the larval fish communities was investigated using the model-based multivariate abundance analysis package 'mvabund' v3.13.1 (Wang et al. 2012). A GLM was fitted to the fish community abundance data using the 'manyglm' function which fits a GLM for each family (10 000 resamples, negative binomial family). The model for the number of fish of family j found at site i (Y_{ij}) is negative binomial:

$$Y_{ij} \sim \mathrm{NB}(\mu_{jkl}, \varnothing_j) \quad (1)$$

where tow i is in location k and at depth treatment l, and log(volume filtered) as an offset. The overdispersion parameter $\varnothing_j$ is constant across sites but can vary across species, and the mean of Y_{ij} is μ_{jkl}, a log-linear function of location, depth, an interaction of location and depth offset by the volume of water filtered:

$$\log(\mu_{jkl}) = \mathrm{intercept}_j + \mathrm{location}_{jk} + \mathrm{depth}_{jl} + \mathrm{location} \times \mathrm{depth}_{jkl} + \mathrm{offset}[\log(\mathrm{volume}_i)] \quad (2)$$

The influence of each species on each of the significant factors (similar to a distance-based SIMPER analysis) was determined using the individual contribution to the sum of the likelihood ratio (sum of LR) (Warton et al. 2012). Homogeneity of variance and model fits were checked by inspecting the residual versus fitted diagnostic plot following Wang et al. (2012) (Fig. S5).

Larval assemblages were visualised using a latent variable model-based unconstrained ordination of the family-level abundances. This model only included

families which had 5 or more larvae observed in total and included volume filtered as an offset. The latent variable ordination was done using the R package 'BORAL' v1.6.1 (Hui 2016).

The zooplankton size-based assemblage was also compared among both eddies and the 2 deeper (MOCNESS) depths using a similar model-based analysis and ordination as described for the larval fish, with zooplankton sizes restricted to 0.2–3.5 mm ESD based upon the resolution of the LOPC. The only difference in the model analysis was that there was no surface depth (due to Triaxus limitations), resulting in only 2 levels of the depth factor. For the transects within each eddy, 5–50 and 50–100 m depth strata were divided into replicates based upon the tow position as it moved in and out of each depth stratum.

2.4. Larval entrainment index

We calculated the entrainment of larval fish spawned in coastal waters (Neira et al. 1998, Gray & Miskiewicz 2000, Gray et al. 2019), relative to the abundance of larval Myctophidae, which is a globally common and abundant oceanic family, composed of 32 genera and over 250 species (Paxton et al. 1984, Paxton & Hulley 1999). Identification of coastal spawning species was based on a review of studies conducted off the east coast of Australia (Smith & Suthers 1999, Gray & Miskiewicz 2000, Keane & Neira 2008, Mullaney et al. 2011, Syahailatua et al. 2011, Mullaney & Suthers 2013, Matis et al. 2014). For studies that sampled both coastal and oceanic waters, the highest larval abundances of the 9 coastal families occurred on the shelf, with lower abundances or absences in samples from oceanic waters. Although larvae of oceanic families such as Myctophidae, Gonostomatidae, Notosudidae and Howellidae were caught in coastal waters, they occurred at much lower abundances compared with the coastal families. Their abundances also usually increased with distance offshore. These relationships with distance were demonstrated by Schilling et al. (2022). The summation of various nearshore larval fish taxa to describe the exchange of coastal water masses with offshore has previously provided a useful metric in the region to measure the impact of upwelling (Smith & Suthers 1999), estuarine recruitment (Ford et al. 2010) and coastal winds (Schilling et al. 2022).

For local coastal spawning taxa in this study, we summed the abundances of 9 families: Sparidae (0.28%); Sillaginidae (0.19%); Carangidae (1.95%); Microcanthidae (0.05%); Cheilodactylidae (0.58%); Labridae (3.48%); Triglidae (0.65%); Platycephalidae 0.39%); and Scorpididae (0.12%), totalling 7.70% of the total larval fish sampled. The index was visualised as a scatterplot where an abundance ratio of coastal taxa/myctophid index value >1 indicated that the assemblage was dominated by coastal taxa while an index value <1 indicated the assemblage was dominated by the oceanic taxa, i.e. in our case, larval myctophids. Both axes on the plot were square root transformed for visualisation. We tested the differences in the larval entrainment index between locations with a GLM including both location and depth as fixed factors and an overall Tweedie distribution. We emphasise that the ratio is a relative index which uses the local abundance of oceanic taxa as the denominator, and the index would change for different studies (depending on the relative abundances of coastal and oceanic taxa).

3. RESULTS

3.1. Water mass properties

The larger cyclonic eddy appeared in sea surface temperature imagery and MODIS-Aqua at ~27.5° S around 9 May 2015 and centered over the slope (Fig. 2A) but shifted offshore within 2 d (Fig. 2B) and remained there (Fig. 2C,D) until sampling on 4 June. The EAC flowed around the eastern and southern perimeter of the eddy and continued southwards along the slope. The eddy had a persistent surface chl *a* concentration of 0.4 mg m^{-3}. The smaller frontal eddy appeared as a billow inshore of the EAC ~2 June at ~31.5° S (Fig. 2E shows 3 June), with a plume of high chl *a* water (>1 mg m^{-3}) entrained offshore (Fig. 2F). By 7 and 8 June (Fig. 2G,H) there was 0.5–0.8 mg m^{-3} surface chlorophyll at the centre of the eddy (32.7° S, 153.3° E).

The temperature and salinity properties of the frontal eddy were distinctive compared to the other locations (Fig. 3). Water in the frontal eddy was cooler and less saline than that in the cyclonic eddy and the 2 coastal locations, over all 3 sampling depths. The frontal eddy surface water and the first 50 m of the water column had temperatures between 20 and 21°C and salinity around 35.55 (Fig. 3A,B). For the same depths, the cyclonic eddy and both coastal locations had temperatures and salinity greater than 21.5°C and 35.6, respectively. Temperature (T) and salinity (S) below the surface were lower for the frontal eddy (T = 19°C, S = 35) and higher for the other locations (T = 19.5–21.5°C, S = 35.55–35.65; Fig. 3C).

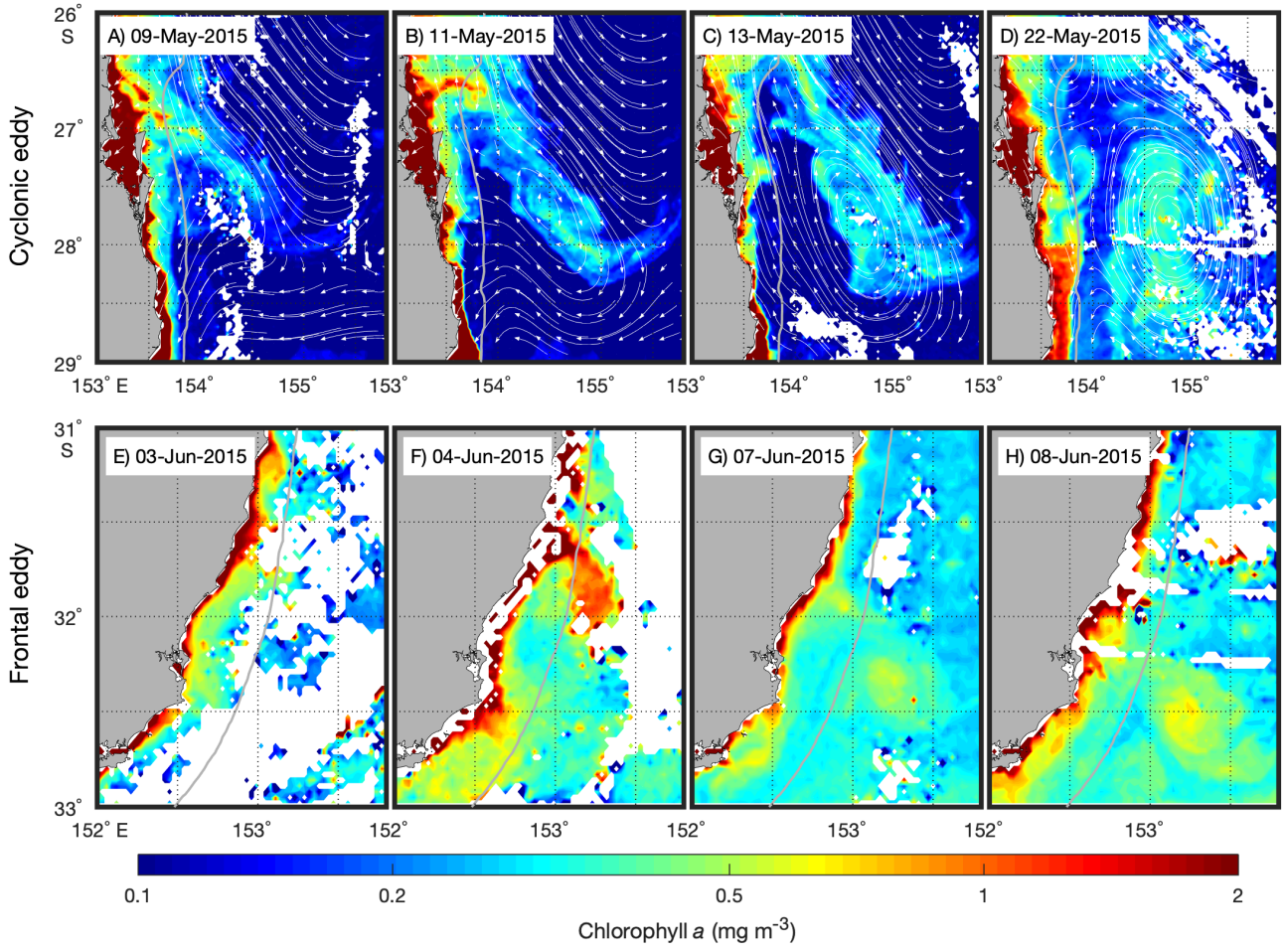

Fig. 2. Remotely sensed images of ocean colour (from MODIS-Aqua) showing the formation and development of (A–D) the northern cyclonic eddy and (E–H) the southern frontal eddy off the east coast of Australia. Note that satellite images were not included in the top row for the period 23 May to 4 June 2015, as they were severely impacted by cloud and do not show the eddy

The thermocline and halocline occurred at approximately 50–60 m depth at all locations (Fig. S6); from more extensive Triaxus tows, Roughan et al. (2017) reported that the mixed layer depth was ~55 m in the core and ~85 m at the edge of both eddies.

3.2. Biological properties

Vertical profiles in fluorescence from the CTD (Fig. S6c) at all 4 locations showed a uniform distribution with depth in the upper mixed layer (<45 m from the surface). In the upper 50 m, there was significantly more chl *a* in the fontal eddy than in the cyclonic eddy, which was greater than the 2 coastal locations (Roughan et al. 2017).

A 160 km north–south transect across most of the cyclonic eddy by the Triaxus (Fig. 1B; Fig. S7), revealed eddy uplift in temperature with the 20°C isotherm rising from 110 m at the eddy edge, to 75 m nearer the centre (black/white contour in Fig. S7). Chl *a* also changed (Fig. S7), associated with steeper NBSS slopes (Fig. S7) and a lower GMS (Fig. S7) in the middle of the eddy. Two transects across the frontal eddy (Fig. 1C; Figs. S8 & S9) show uplift in the isotherms, and steeper NBSS slopes and smaller GMS.

3.3. Larval fish community

A total of 38 899 fish larvae was caught, representing 101 families (Table S1). Myctophidae composed 48% of the community, followed by Notosudidae (10%), Labridae (3.5%) and Phosichthyidae (3.4%). The other families all had abundances <3% of the total (Table S1). Overall, there was a high abundance of larval fish (mostly myctophids) in the Coast–S

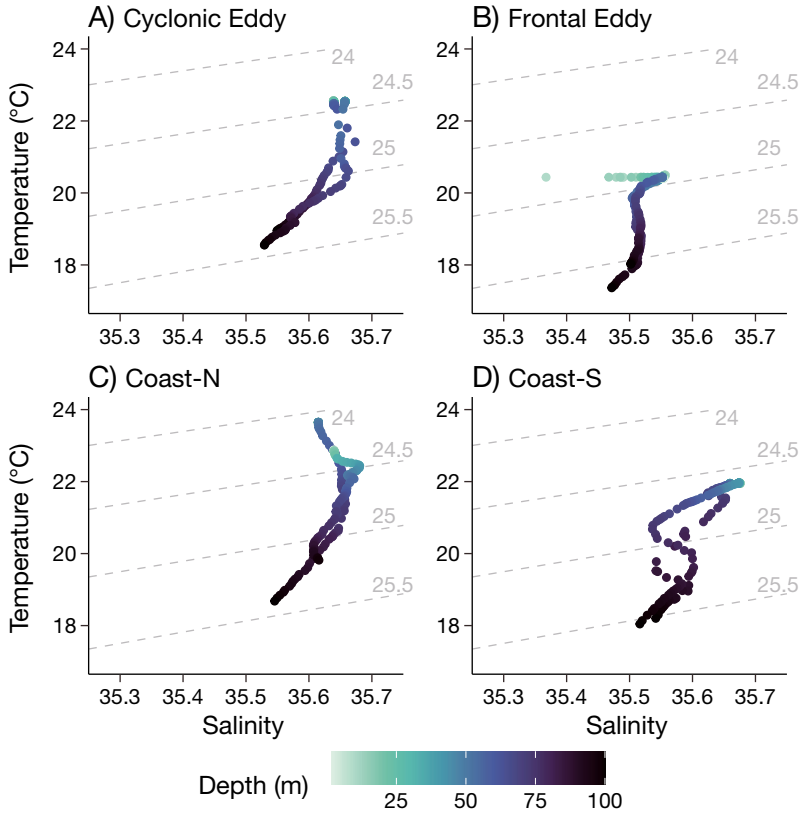

Fig. 3. Temperature–salinity plots from the CTD, restricted to the top 100 m for each site. There were 2 CTD casts at each location and each dot represents a 1 m depth bin. The light grey dashed lines show the isopycnals

region and the cyclonic eddy (Fig. 4A), which was significantly different from the frontal eddy, where the lowest overall abundance was recorded ($p < 0.05$; Fig. 4A). For the other families combined, the highest abundances occurred at the 5–50 m depth stratum and the lowest at the 50–100 m depth stratum (Fig. 4B). In terms of diversity, the frontal eddy was the most diverse, followed by Coast–N, cyclonic eddy and Coast–S (Fig. 4C).

Shannon's index of diversity varied significantly depending on location and depth (2-way ANOVA, $F_{6,81} = 6.321$, $p < 0.001$, Fig. 4C). The abundance of Myctophidae also varied among location and depth (GLM, $\chi^2_6 = 28.512$, $p < 0.001$, Fig. 4A), as did the abundance of other taxa (GLM, $\chi^2_6 = 12.974$, $p = 0.043$, Fig. 4B). Total abundance varied between locations (GLM, $\chi^2_3 = 25.547$, $p < 0.001$) and depths (GLM, $\chi^2_2 = 29.009$, $p < 0.001$, Fig. 4D), but there was no evidence of a significant interaction (GLM, $\chi^2_6 = 9.254$, $p = 0.160$).

These significant differences are evident in the latent variable ordination plot (Fig. 5) and are consistent with the community composition changing with both location and depth (Figs. S10 & S11; Multivariate Generalised Linear Model, Dev = 911.38, p = 0.001). The families associated with the arrows in Fig. 5 are indicators for each water mass. Myctophidae and other oceanic taxa (Notosudidae, Phosichthyidae, Howellidae and Gonostomatidae) were present at all locations, but with a lower percentage contribution in the frontal eddy. The frontal eddy was distinguished by coastal families, with Cheilodactylidae, Carangidae, Gonorhynchidae and Platycephalidae being the main contributors to differences in the assemblage (Table 1; Figs. S10 & S11). Cyclonic eddy stations were distinguished by the oceanic Notosudidae and coastal and coral reef families with the main contributors being Scaridae, Scorpaenidae and Cirrhitidae. The oceanic Notosudidae, Phosichthyidae, Howellidae and Gonostomatidae represented 23 and 35% of the cyclonic eddy and Coast–S assemblages, respectively. The coastal Clupeidae and Engraulidae, and oceanic Melanostomiinae were more common at Coast–N stations (Table S1, Figs. S10 & S11).

Myctophidae, Notosudidae and Labridae were distributed across all 3 depths. Scomberesocidae, Gonorhynchidae and Sparidae characterised the 0–5 m samples. The 5–50 m depth was characterised by Engraulidae, Myctophidae and Howellidae. The 50–100 m depth bin had a lower abundance of most taxa and was only characterised by Acropomatidae (Table 2; Figs. S11 & S12).

3.4. Zooplankton biomass and size structure

The biomass of zooplankton derived from the LOPC revealed less biomass in the frontal eddy (188 and 57 mg m^{-3} over the same 2 depth strata sampled by the MOCNESS; 5–50 and 50–100 m depth strata, respectively, Fig. 6A), compared to the cyclonic eddy (264 and 154 mg m^{-3} for shallower and deeper depths, respectively, Fig. 6B). The corresponding NBSSs revealed a shallower slope in the frontal eddy 5–50 m depth stratum (NBSS slope = –0.89, Fig. 6A), compared to that observed in the 50–100 m depth stratum (NBSS slope = –0.95), and the northern cyclonic

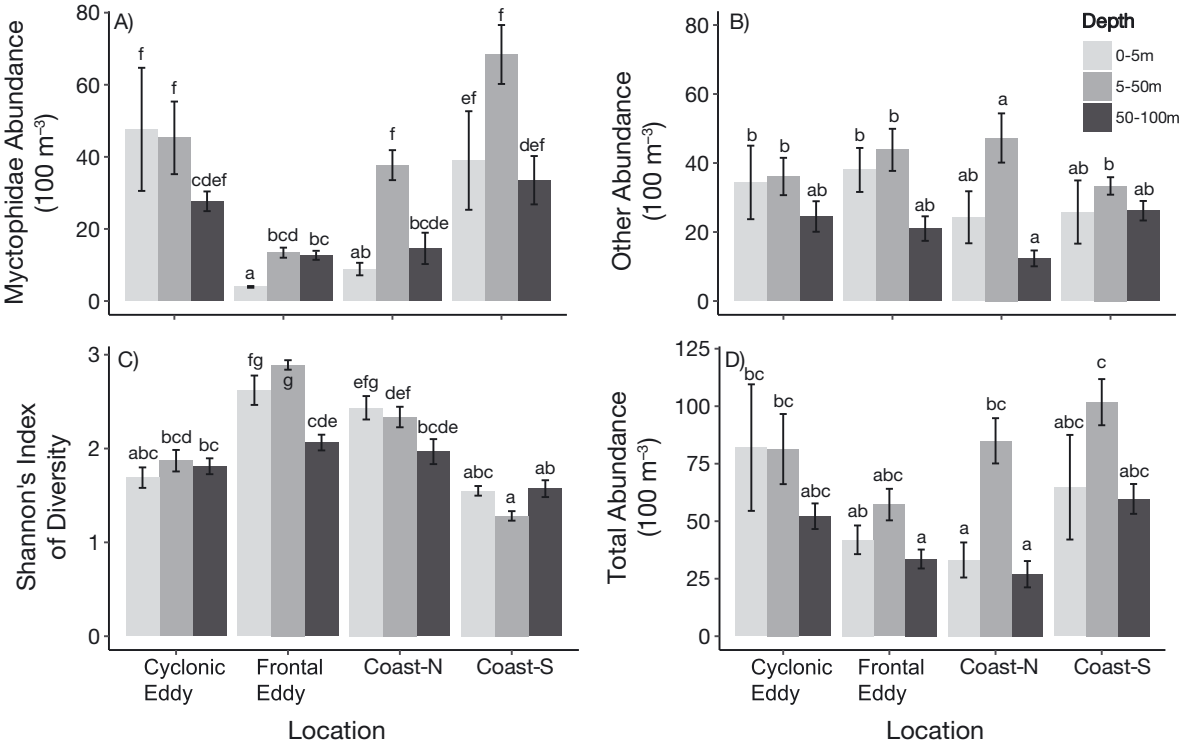

Fig. 4. Summary plot of larval fish communities at the 4 study sites/locations: (A) abundance of Myctophidae, (B) abundance of other larval fish, (C) diversity and (D) total abundance of all larval fish. Within each subplot, bars that do not share a common letter are significantly different ($p < 0.05$)

eddy (NBSS slope= −0.98, −0.97 for shallower and deeper depth strata, respectively, Fig. 6B).

The zooplankton biomass size structure obtained from the LOPC and Triaxus (Fig. 7) readily differentiated both eddies. When visualised as an ordination, the vertical axis distinguished the zooplankton based on biomass with least biomass in the frontal eddy, especially at depth (50–100 m). The horizontal axis contrasted the small particles <300 µm evident in the cyclonic eddy (e.g. production of nauplii and small copepods, 215–293 µm ESD) with larger particles 1–3 mm ESD (e.g. small krill, Syahailatua et al. 2011) found in the frontal and cyclonic eddies. These larger particles are also evident in the size spectra (Fig. 6).

3.5. Larval entrainment index

The initial entrainment and temporal changes in the coastal larval assemblage were assessed relative to the abundance of larval Myctophidae, an abundant oceanic family (Fig. 8). Expressed as a ratio, in the southern frontal eddy the mean abundance ratio of coastal/myctophid larvae was 11.0 (range 2.2–27.7), while in the northern cyclonic eddy, the ratio was less than half (2.90–5.2; Fig. S13). This coastal assemblage primarily occurred in the 0–5 and 5–50 m depth strata of the frontal eddy and exceeded the abundance of larval myctophids (Fig. 4). The coastal assemblage was approximately half the abundance of larval myctophids at the 50–100 m depth of the frontal eddy, and in the surface and 50–100 m depth stratum of Coast–N. The northern cyclonic eddy and especially Coast–S (the coastal location flooded by the EAC) were dominated by larval myctophids and other oceanic taxa (Fig. 4A). The GLM analysis provides strong evidence for differences in larval entrainment index among locations and depths (location × depth interaction: $\chi^2_6 = 29.6$, $p < 0.001$). Post-hoc tests revealed the frontal eddy entrainment index was very clearly different from all other location and depth combinations ($p < 0.001$) except for the 50–100 m frontal eddy showing no difference to the surface samples from Coast–N ($p = 0.998$; Fig. 8).

4. DISCUSSION

The larval fish and zooplankton assemblages found in 2 different cyclonic eddies revealed some dynamic processes of their recent history. The frontal eddy was a small, rapidly rotating feature that began

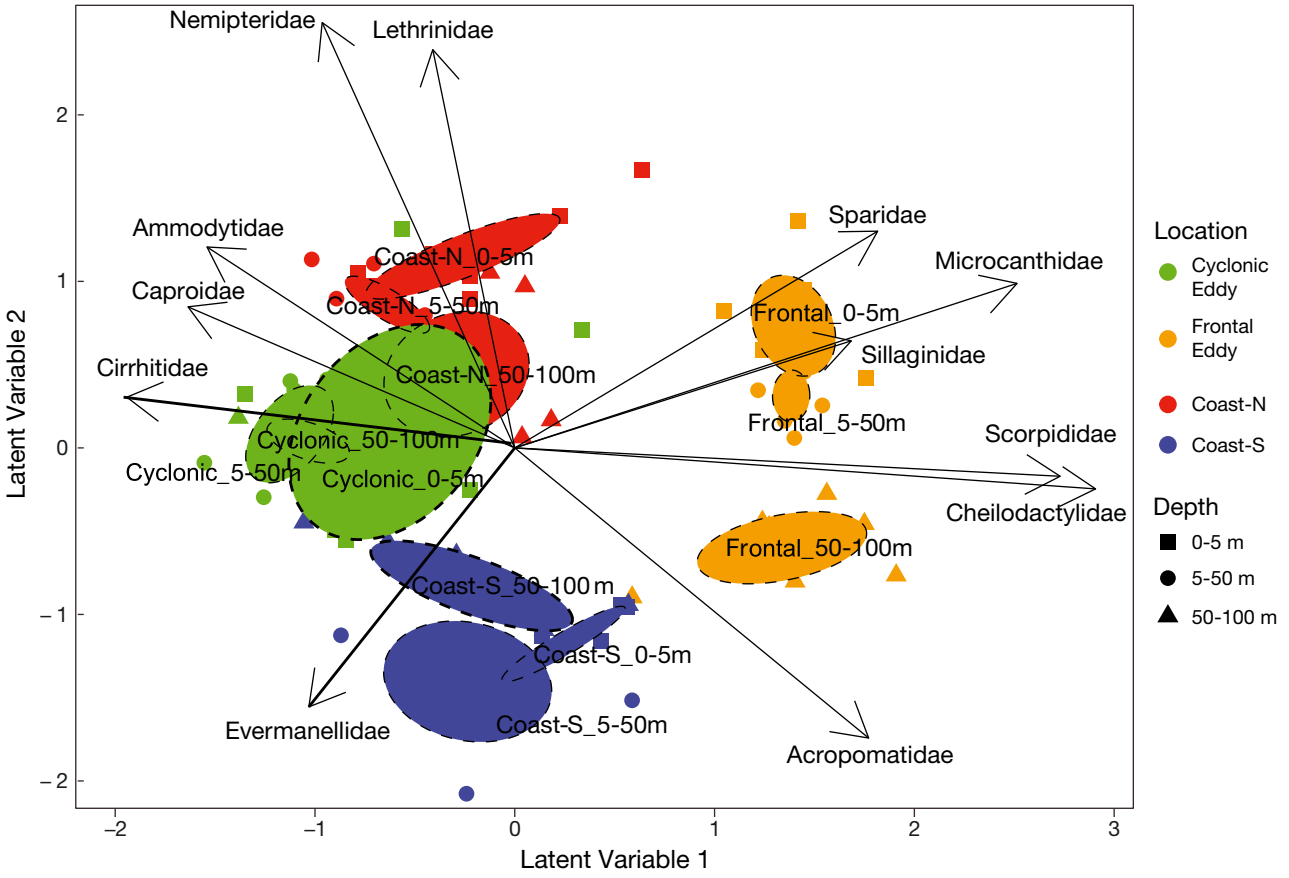

Fig. 5. Latent variable model-based ordination plot of larval fish assemblages in relation to the sites (colours) and depths (shapes). The 12 taxa with the largest latent variable coefficients are shown. Ellipses show the 95% confidence region of the mean for each location–depth combination. Note the frontal eddy has entrained coastal taxa and shifted offshore, causing the putative location of entrainment at Coast–S to be exchanged with oceanic water

as a billow of the EAC frontal edge, entraining the shelf waters in a process similar to that described by Everett et al. (2015), which quickly transported these waters off the shelf (Roughan et al. 2017). In contrast, the northern cyclonic eddy was older, with a 5-fold greater diameter which had interacted with the shelf and entrained some coastal taxa. Such eddies are a pervasive component of most western boundary cur-

Table 1. Summary of the % sum of likelihood ratio (LR) analysis (SIMPER equivalent) comparing locations (see Fig. 1). Only the top 12 most influential taxa as identified by the % sum of LR method are shown (Warton et al. 2012)

Taxon	Mean abundance (ind. m^{-3})				LR statistic	% Sum of LR
	Cyclonic eddy	Frontal eddy	Coast–N	Coast–S		
Cheilodactylidae	0.01	1.30	0.01	0.00	85.44	4.02
Notosudidae	12.41	0.97	2.56	9.92	70.84	3.33
Carangidae	0.19	3.78	0.52	0.10	64.23	3.02
Melanostomiinae	0.36	0.06	1.34	0.17	56.84	2.67
Triglidae	0.00	0.94	0.21	0.34	54.06	2.54
Scaridae	1.19	0.05	0.26	0.14	53.75	2.53
Myctophidae	40.73	9.97	20.39	47.69	50.58	2.38
Howellidae	1.32	0.40	0.50	3.76	49.82	2.34
Clupeidae	0.05	0.47	1.96	0.11	48.33	2.27
Gempylidae	0.57	0.09	0.77	0.53	48.07	2.26
Lethrinidae	0.03	0.01	0.77	0.00	47.88	2.25
Sparidae	0.00	0.60	0.05	0.01	47.87	2.25

Table 2. Summary of the % sum of likelihood ratio (LR) analysis (SIMPER equivalent) comparing the 3 depth strata. Only the top 12 most influential taxa as identified by the % sum of LR method are shown (Warton et al. 2012)

Taxon	Mean abundance (ind. m^{-3})			LR test statistic	% Sum of LR
	Surface (0–5 m)	5–50 m	50–100 m		
Scomberesocidae	2.06	0.02	0.03	67.17	5.85
Clupeidae	0.95	1.02	0.03	53.82	4.69
Engraulidae	0.32	1.38	0.04	41.02	3.57
Gonorhynchidae	3.96	0.45	0.04	40.57	3.53
Nomeidae	0.42	0.46	0.08	35.82	3.12
Sparidae	0.32	0.19	0.01	34.95	3.04
Astronesthinae	0.36	0.32	0.04	34.75	3.03
Mullidae	0.73	0.48	0.08	28.39	2.47
Howellidae	1.26	2.28	0.78	28.10	2.45
Acropomatidae	0.15	1.34	3.10	25.07	2.18
Melanostomiinae	0.47	0.83	0.15	25.01	2.18
Schindleridae	0.02	0.16	0.05	21.14	1.84

rents (Nakata et al. 2000, Everett et al. 2012, Govoni et al. 2013, Oke et al. 2019), and an essential component for understanding population connectivity of coastal ecosystems in a changing ocean climate. Of particular interest is when eddies interact with the shelf waters and entrain fish and invertebrate larvae from the productive continental shelf. This entraining process is physically and biologically complex, involving an inward spiral of shelf water to a depth of neutral buoyancy (Everett et al. 2015), coupled with the dynamic processes of larval growth, mortality and development. We summarised the outcome of these complex spatio-temporal processes with the larval entrainment index (Fig. 8), and we suggest this index could be applied to other studies of cross-shelf flows, eddy transport and population connectivity.

4.1. Entrainment and development of larval fish assemblages

Our voyage originally intended to examine the implications of eddy entrainment by comparing the larval fish assemblage in the 2 eddies with the approximate 'source' waters originating on the shelf. However, the southern coastal waters and the frontal eddy effectively exchanged their larval assemblages, as EAC water was pulled onto the shelf when the frontal eddy moved offshore. The rapid exchange of coastal water mass was observed elsewhere to occur within a day, in response to coastal winds or oceanographic upwelling (Smith & Suthers 1999), but this effect of a frontal eddy has not been observed before. Others have shown that the assem-

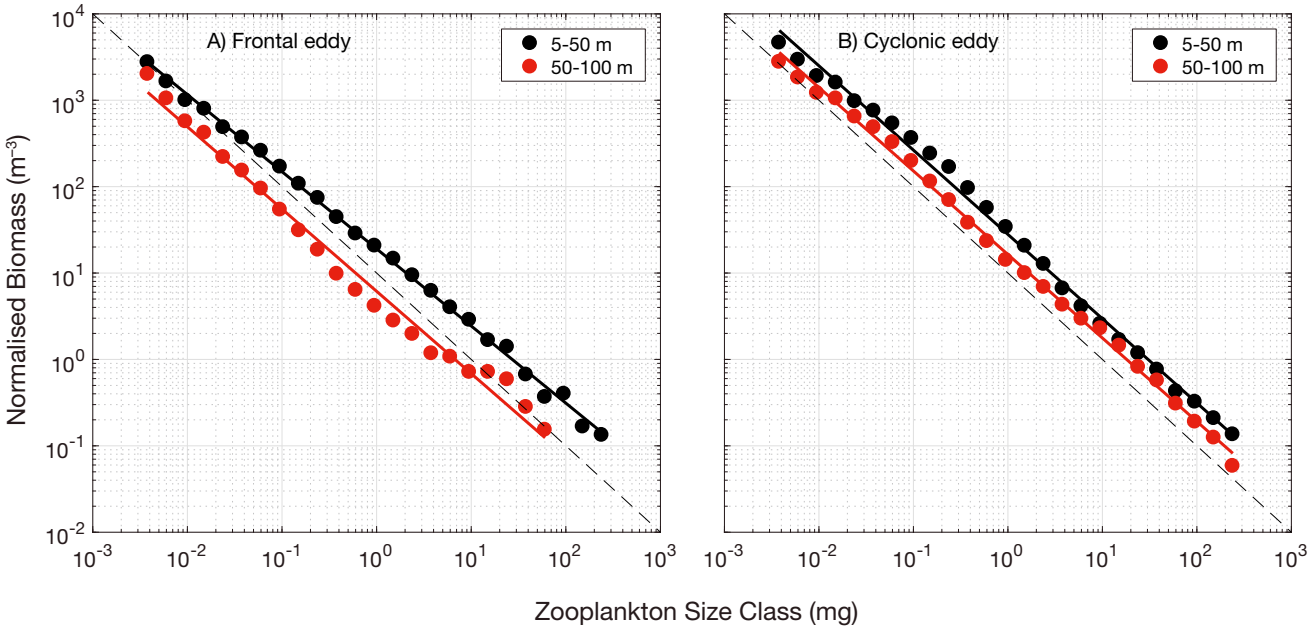

Fig. 6. Normalised biomass size spectrum from Triaxus transects supporting the laser optical plankton counter in (A) the southern frontal eddy (see Fig. 1C) and (B) the northern cyclonic eddy (see Fig. 1B) for 5–50 and 50–100 m depths; depth bins correspond to the 2 MOCNESS depth strata. Horizontal axis is centred around 1 mg (1.49 mm equivalent spherical diameter [ESD], with a range of 0.001–1000 mg [0.15–14.9 mm ESD]). The dashed black line shows a reference line of slope −1 where zooplankton mortality is balanced by growth

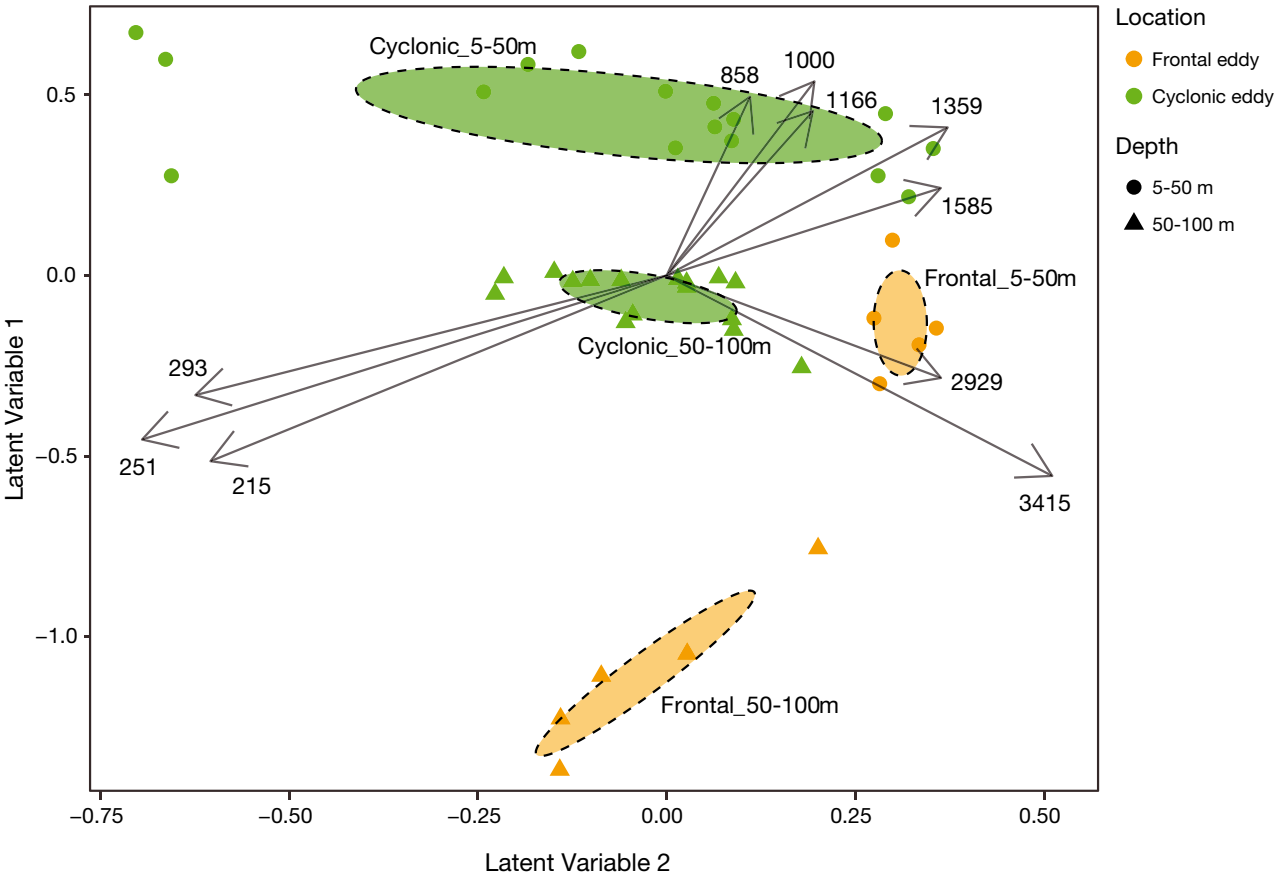

Fig. 7. Latent variable model-based ordination plot of zooplankton biomass size categories (n = 19 size bins) in relation to the 2 eddies (frontal and cyclonic) and the 2 deeper depths (5–50 and 50–100 m depth strata) using Triaxus-LOPC data, geometric mean equivalent spherical diameter (ESD) 215–3415 µm. The vectors describing the top 10 most influential size categories are shown (at the end of each vector is the geometric mean ESD of each size bin, µm). Ellipses show the 95% confidence region of the mean for each location–depth combination

blage structure of an eddy was correlated with the geographic area where it is formed (Atwood et al. 2010). Waite et al. (2007) also showed how anticyclonic eddies of the Leeuwin Current entrained phytoplankton assemblages of coastal water. Several studies of warm and cold core rings in the Gulf Stream system show entrainment and transport of coastally spawned larval fish communities (Hare & Cowen 1996, Govoni et al. 2013, Shulzitski et al. 2018). Similarly, in the Canary Current upwelling system off NW Africa, cross-shelf larval fish assemblages interact with mesoscale eddies (Moyano et al. 2014, Olivar et al. 2016, Tiedemann et al. 2018). The Canary Current surveys showed a marked cross-shelf transition of larval assemblages from coastal to oceanic-dominated assemblages from the coast to offshore. Coastal species were found to accumulate in eddies, which could enhance growth and survival and facilitate retention, before their subsequent return to coastal juvenile habitats.

The southern frontal eddy contained a distinctive coastal/estuarine opportunist larval assemblage of commercially important Sparidae, Sillaginidae, Cheilodactylidae and Platcephalidae and the larvae of taxa typical of rocky reefs (Microcanthidae and Scorpididae). Typically, these species spawn off surf beaches and in the inner shelf (Gray et al. 2019, Gray & Miskiewicz 2000). Within days of the frontal eddy forming, however, the adjacent coastal waters were entirely replaced by warmer, saltier water of the EAC and the corresponding oceanic larval assemblage. This stark contrast was evident in the temperature–salinity plots (Fig. 3) and in the multivariate larval assemblages (Fig. 5). Unfortunately, we have no knowledge of the original coastal assemblage at the time of entrainment, 7 d before we sampled the frontal eddy, but presumably it was similar to the frontal eddy with a high proportion of coastal taxa. The low salinity spike in the surface waters (Fig. S6) suggests the frontal eddy even entrained estuarine

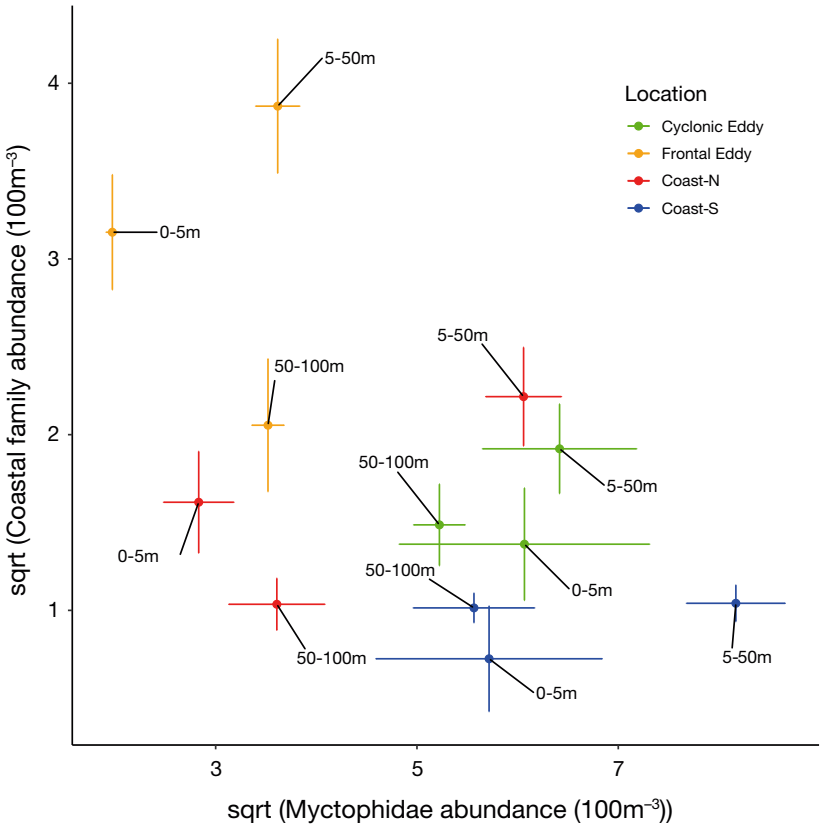

Fig. 8. Larval entrainment index shown as the averaged, summed abundance of 9 coastal taxa (Sparidae, Sillaginidae, Carangidae, Microcanthidae, Cheilodactylidae, Labridae, Triglidae, Platycephalidae and Scorpididae), plotted on the abundance of larval lanternfish (Myctophidae), the most abundant oceanic taxon in this study. Data are square-root (sqrt) transformed. Data points towards the upper left reveal significant entrainment of coastal larvae. Data points are colour coded by the 4 locations (see Fig. 1), and labelled with the 3 tow-depth strata (0–5, 5–50, 50–100 m). Error bars are standard error

plume water and that this eddy assemblage likely reflects the original coastal source.

Therefore due to EAC influence, the Coast–S assemblage was the most oceanic of all 4 locations in terms of temperature–salinity in the surface and upper mixed layer, and in terms of the predominance of oceanic Myctophidae and Notosudidae larvae. In contrast, the older cyclonic eddy and adjacent Coast–N were dominated by a variety of oceanic and coastal taxa. The Coast–N location was also influenced by the EAC, located near the shelf break. The surface waters of the northern cyclonic eddy consisted of Subtropical Lower Water of the EAC (Roughan et al. 2017), as the warmer EAC waters had flooded over the lower sea level of the cyclonic eddy. Surface flooding of cooler, denser eddies is a known feature in the EAC system (Baird et al. 2011).

We used the larval entrainment index to compare the abundances of 9 dominant coastal taxa in relation to the larval Myctophidae abundance (Fig. 8). Similar relationships were evident if we used on the abscissa the abundance of other common oceanic families such as Notosudidae or Phosichthyidae. Consistent with the temperature–salinity properties and modelling (Everett et al. 2015), this plot revealed the highest abundance of coastal taxa in the frontal eddy 0–5 m and 5–50 m depth bins. At the other extreme, the Coast–S location, which was flooded by EAC water, proportionally had the lowest abundance of coastal taxa in all depth bins. This relationship also revealed that the Coast–N had a greater proportion of coastal taxa compared with the cyclonic eddy which only had a few coastal taxa. We expected that with time, the index would change due to growth and mortality of the entrained larvae and the coastal assemblage would effectively become diluted. We tried to test this expectation, by returning to the frontal eddy after ~7 d using the position of the one remaining drifter on ~16 June (Roughan et al. 2017). However, bad weather, cloud cover and flooding by warmer EAC water prevented sampling. At this stage after 2 wk of formation, the frontal eddy was more than 400 km from the coast, with the centre moving approximately 17 km d^{-1} to the east–southeast. While this eddy advection was significantly less than the EAC flow (Roughan et al. 2017), its trajectory suggested it was transporting coastal larvae further away from the coast. The behaviour of this small and rapidly moving frontal eddy is in contrast to others we have sampled, which tend to either roll along the slope and frontal EAC edge (Everett et al. 2012), or become topographically trapped and grow where the EAC separates from the coast in the western Tasman Front (Mullaney et al. 2014, Oke et al. 2019). In the case of this particular frontal eddy, the larval advection offshore may be a loss to the coastal fish community. Alternatively, others have observed that returning flow to the coast is driven by eddy jets in the region (Cetina-Heredia et al. 2019a, Malan et al. 2020), and that temperate reef fish larvae have good swimming capacity to return to the coast (Downie et al. 2021).

The depth distribution of larval fish, especially that of the important coastal taxa, was of particular interest (Hawes et al. 2020) in relation to the mechanism modelled by Everett et al. (2015). Their study revealed that cooler coastal waters from southern latitudes sank once they were entrained into the frontal eddy. The key is the density of the entraining coastal waters relative to the eddy, which may be influenced by warmer EAC water. It is possible that if larvae are entrained too deep it may affect their survival, and/or not be quantified by our typical near-surface sampling strategy (e.g. Matis et al. 2014). In the present study, we found that the frontal eddy entrained the coastal assemblage into the surface and upper mixed layers of the eddy (~50 m), consistent with that modelled by Everett et al. (2015), and relatively few larvae were found in the deeper 50–100 m depth bin. It would be interesting, therefore, to determine the implications of entrainment of more dense coastal waters into a warm-core eddy, which should result in larval fish sinking to well over 100 m deep. This may explain why warm core eddies, even those that clearly interact with the shelf (Matis et al. 2014), appear to have so few coastally important taxa in the upper mixed layer. Alternatively, the elongation of the eddy can reduce retention of water (Cetina-Heredia et al. 2019b). Hawes et al. (2020) investigated the size and stage-dependent vertical migration patterns in larvae of 7 families of temperate reef fish in these same eddies. Larvae of 4 families exhibited a downward migration with ontogeny. In addition, for 6 of the 7 families, larvae inside the eddy were longer compared with those in coastal waters, suggesting larval retention and growth.

4.2. Caveats to the larval entrainment index

Inner shelf waters adjacent to western boundary currents are usually pre-conditioned by upwelling with enriched chlorophyll biomass (e.g. Everett et al. 2014, 2015) and more abundant ichthyoplankton (Mullaney et al. 2011). The relative mixing of coastal and oceanic larval fishes could be assessed at other study areas using a larval entrainment index, providing that there is a diverse assemblage of coastal larval taxa in the samples. However, the index will decline during the days and weeks after the entrainment event, as coastal larvae either develop in length and swimming ability, increasing net avoidance, or they may die out, while oceanic larvae continue to recruit to the eddy. Use of this index relies on local knowledge of coastal fish diversity, both of their reliable identification and known spawning habitats. The index may be affected by vertical migration of different taxa, which is why we conducted all of our sampling at night. The index is only a relative index for comparison within a voyage and cannot be compared among studies unless larval abundances are standardised for each study (e.g. Schilling et al. 2022). It would be interesting to compare a variety of standardised datasets, to determine how different sized or located eddies may cause different degrees of entrainment. Notably, even the northern cyclonic eddy had some coastal larvae, even though it had not physically interacted with the shelf for several weeks. The denominator, i.e. the myctophids, was based on their abundance, as they dominated the overall diversity (48% of all individuals). We could use other abundant taxa such as notosudids, gonostomatids or howellids, or any other characteristic oceanic larval taxon or a combination of taxa and the results would be consistent (although these other taxa are not as diverse as the myctophids).

It may be possible that the entrainment index could be skewed by the spawning phenology of a particular group — for example, that larval myctophid fishes could swamp the ratio during a spawning event and obscure a significant entrainment event. Clearly, the coastal and oceanic abundances should be inspected *a priori* for such an event. In general, however, the index should be robust to the stochastic effects of spawning phenology by the diversity of coastal and myctophid fishes and their diverse spawning behaviours, particularly in the context of a relative index for comparisons within a study. For example, Gray & Miskiewicz (2000) repeatedly sampled multiple stations 14 times on the shelf over a 4 yr period. For the 9 families of coastal larvae, 7 were recorded in 12–14 of the sampling events while the other 2 were caught 7 and 9 times. This indicates extended spawning periods, but with peak abundances of different families varying seasonally. In these samples, myctophid larvae were caught in all 14 sampling events but with a marked variation in seasonality, with higher abundances in autumn and winter compared with spring and summer.

We sampled only 4 stations at each location, and it is likely that the larger northern cyclonic eddy was more complex with greater patchiness (spatial variability; Fig. 1) than we could determine on the voyage. However, the Triaxus profiles covered a longer distance and confirmed that our stations were on the western side of the eddy. Furthermore, the larval entrainment index analysis showed strong evidence and strong effect size for differences among

locations (Fig. 8; Fig. S13), suggesting that our general conclusions are robust.

4.3. Zooplankton biomass and size structure

The younger frontal eddy with its assemblage of coastal fish larvae had only ~50% of the zooplankton biomass compared to the older cyclonic eddy. This was surprising, compared to other studies of entrainment of pre-conditioned shelf water into upwelling favourable frontal eddies. For example, compared to the surrounding waters, Mullaney & Suthers (2013) observed a distinctive bulge in the zooplankton NBSS, composed of young krill and salps. However, the study by Mullaney & Suthers (2013) was conducted during the spring, whereas our present study took place in early winter when coastal waters were cooler relative to offshore, which may have reduced production and planktonic biomass. The slope of the biomass size spectrum summarises the mortality/growth ratio of the zooplankton and ichthyoplankton (Suthers et al. 2021). The flatter slope of the size spectrum in the frontal eddy indicates more efficient energy transfer (where there is more growth and/or less mortality) than in the other 3 locations, as also observed in other frontal eddies (Mullaney & Suthers 2013). Therefore, the larval fish assemblage of the frontal eddy would also experience better survival, assuming that zooplankton responds similarly to ichthyoplankton.

It is possible that the deeper 50–100 m depth bin of the frontal eddy may approximate the initial conditions on the shelf, which over the 7 d of eddy formation elevated the NBSS in the shallower depth bin (5–50 m). In comparison, the larger cyclonic eddy showed double the zooplankton biomass, probably because it was warmer offshore and had ~4 wk more time for secondary production to accumulate. Furthermore, the shallower depth bin (5–50 m) had nearly double the biomass of the deeper depth bin (50–100 m). Kwong et al. (2020) sampled the mesozooplankton at 100 m intervals down to 500 m in the centre and at the edge of the cyclonic eddy. They found that the day and night mesozooplankton biomass was significantly different in the centre, with no difference detected at the edge. Biomass was also generally higher at night than during the day. Being upwelling favourable, the eddy had the time (~4 wk) to generate new zooplankton biomass compared to the surrounding waters (Baird et al. 2006).

The composition of the planktonic assemblage in the eddy will change with time due to growth and mortality, supplemented by further larval recruitment by myctophids and larvae of other oceanic families. Sometimes larval entrainment offshore is considered a loss to the coastal ecosystem (Waite et al. 2007, Nieto et al. 2014) or alternatively, it has the potential to be an offshore nursery (Kasai et al. 2002, Mullaney & Suthers 2013), before juveniles return to estuarine and coastal nursery habitats through eddy-driven transport (Cetina-Heredia et al. 2019a, Malan et al. 2020), or active swimming across the shelf. Similar processes such as streamers from anticyclonic eddies in the Gulf Stream are capable of transporting larval bluefish *Pomatomus saltatrix* back to the coast from spawning areas off Florida (Hare & Cowen 1996), a process which likely occurs within the EAC (Schilling et al. 2020). These alternative outcomes should be tested with an analysis of both larval growth and mortality between the shelf and offshore habitats. The effect of eddy behaviour and the fate of frontal eddies should also be resolved, such as with high-resolution, data-assimilating oceanographic models (Kerry et al. 2018).

Acknowledgements. We thank the CSIRO Marine National Facility (MNF) for its support in the form of sea time on RV 'Investigator' (voyage IN2015_V03), support personnel, scientific equipment and data management. All data and samples acquired on the voyage are made publicly available in accordance with MNF policy (https://www.cmar.csiro.au/data/trawler/). During this commissioning year voyage we experienced some significant technical challenges that were professionally managed by the master Mike Watson, and voyage managers Max MacGuire and Don McKenzie, and a very supportive crew. We are grateful for the extra efforts by the science support team (Brett Muir, Aaron Tyndall, Mark Lewis), the swath and computing team Hugh Barker, Stewart Wilde, Dave Watts and Matt Boyd, and the hydrochemists Mark Reyner, Cassie Schwanger and Christine Rees, who made this voyage a success. We also thank our colleagues on the voyage including Lian Kwong, Brian Griffiths and Martina Doblin and the Blue Team. V.G. acknowledges financial support provided by Coordenação de Aperfeiçoamento de Pessoal de Nível Superior (CAPES) and Programa de Doutorado Sanduíche no Exterior (PDSE) (process 3416/15-1). J.D.E. was supported by an Australian Research Council DP150102656, and operational funds by the University of New South Wales. The Blue Team were partially funded by Australian Research Council LP 150100064 to M.R. This research is a contribution to the World University Worldwide Universities Network project; Ocean Eddies in a Changing Climate: Understanding the Impact of Coastal Climates and Fisheries Production. This is contribution number 285 from the Sydney Institute of Marine Science. MODIS and AVHRR satellite data were sourced as part of the Integrated Marine Observing System (IMOS), which is supported by the Australian Government through the National Collaborative Research Infrastructure Strategy.

LITERATURE CITED

Atwood E, Duffy-Anderson JT, Horne JK, Ladd C (2010) Influence of mesoscale eddies on ichthyoplankton assemblages in the Gulf of Alaska. Fish Oceanogr 19:493–507

Baird ME, Timko PG, Suthers IM, Middleton JH (2006) Coupled physical–biological modelling study of the East Australian Current with idealised wind forcing: Part II. Biological dynamical analysis. J Mar Syst 59:271–291

Baird ME, Suthers IM, Griffin DA, Hollings B and others (2011) The effect of surface flooding on the physical–biogeochemical dynamics of a warm-core eddy off southeast Australia. Deep Sea Res II 58:592–605

Bakun A (2006) Fronts and eddies as key structures in the habitat of marine fish larvae: opportunity, adaptive response and competitive advantage. Sci Mar 70:105–122

Booth DJ, Figueira WF, Gregson MA, Brown L, Beretta G (2007) Occurrence of tropical fishes in temperate southeastern Australia: role of the East Australian Current. Estuar Coast Shelf Sci 72:102–114

Cetina-Heredia P, Roughan M, Liggins G, Coleman MA, Jeffs A (2019a) Mesoscale circulation determines broad spatio-temporal settlement patterns of lobster. PLOS ONE 14:e0211722

Cetina-Heredia P, Roughan M, van Sebille E, Keating S, Brassington GB (2019b) Retention and leakage of water by mesoscale eddies in the East Australian Current system. J Geophys Res Oceans 124:2485–2500

Downie AT, Leis JM, Cowman PF, McCormick MI, Rummer JL (2021) The influence of habitat association on swimming performance in marine teleost fish larvae. Fish Fish 22:1187–1212

Everett JD, Baird ME, Oke PR, Suthers IM (2012) An avenue of eddies: quantifying the biophysical properties of mesoscale eddies in the Tasman Sea. Geophys Res Lett 39:L16608

Everett JD, Baird ME, Roughan M, Suthers IM, Doblin MA (2014) Relative impact of seasonal and oceanographic drivers on surface chlorophyll *a* along a Western Boundary Current. Prog Oceanogr 120:340–351

Everett JD, Macdonald H, Baird ME, Humphries J, Roughan M, Suthers IM (2015) Cyclonic entrainment of preconditioned shelf waters into a frontal eddy. J Geophys Res Oceans 120:677–691

Ford JR, Williams RJ, Fowler AM, Cox DR, Suthers IM (2010) Identifying critical estuarine seagrass habitat for settlement of coastally spawned fish. Mar Ecol Prog Ser 408:181–193

Govoni JJ, Hare JA, Davenport ED (2013) The distribution of larval fishes of the Charleston Gyre region off the southeastern United States in winter shaped by mesoscale, cyclonic eddies. Mar Coast Fish 5:246–259

Gray CA, Miskiewicz AG (2000) Larval fish assemblages in south-east Australian coastal waters: seasonal and spatial structure. Estuar Coast Shelf Sci 50:549–570

Gray CA, Miskiewicz AG, Otway NM, Kingsford MJ (2019) Historical daytime vertical structure of larval fish assemblages in southeast Australian coastal waters: a benchmark for examining regional ecosystem change. Reg Stud Mar Sci 29:100634

Hardman-Mountford NJ, Richardson AJ, Boyer DC, Kreiner A, Boyer HJ (2003) Relating sardine recruitment in the Northern Benguela to satellite-derived sea surface height using a neural network pattern recognition approach. Prog Oceanogr 59:241–255

Hare JA, Cowen RK (1996) Transport mechanisms of larval and pelagic juvenile bluefish (*Pomatomus saltatrix*) from South Atlantic Bight spawning grounds to Middle Atlantic Bight nursery habitats. Limnol Oceanogr 41:1264–1280

Hartig F (2020) DHARMa: residual diagnostics for hierarchical (multi-level/mixed) regression models. R package version 0.3.3.0. https://CRAN.R-project.org/package=DHARMa

Hawes S, Miskiewicz A, Garcia V, Figueira W (2020) Size and stage-dependent vertical migration patterns in reef-associated fish larvae off the eastern coast of Australia. Deep Sea Res I 164:103362

Herman AW, Beanlands B, Phillips EF (2004) The next generation of Optical Plankton Counter: the Laser-OPC. J Plankton Res 26:1135–1145

Hinchliffe C, Pepin P, Suthers IM, Falster DS (2021) A novel approach for estimating growth and mortality of fish larvae. ICES J Mar Sci 78:2684–2699

Holliday D, Beckley LE, Olivar MP (2011) Incorporation of larval fishes into a developing anti-cyclonic eddy of the Leeuwin Current off south-western Australia. J Plankton Res 33:1696–1708

Hui FKC (2016) BORAL — Bayesian ordination and regression analysis of multivariate abundance data in R. Methods Ecol Evol 7:744–750

Hui FKC, Taskinen S, Pledger S, Foster SD, Warton DI (2015) Model-based approaches to unconstrained ordination. Methods Ecol Evol 6:399–411

Kasai A, Kimura S, Nakata H, Okazaki Y (2002) Entrainment of coastal water into a frontal eddy of the Kuroshio and its biological significance. J Mar Syst 37:185–198

Keane JP, Neira FJ (2008) Larval fish assemblages along the south-eastern Australian shelf: linking mesoscale non-depth-discriminate structure and water masses. Fish Oceanogr 17:263–280

Kerry C, Roughan M, Powell B (2018) Observation impact in a regional reanalysis of the East Australian Current system. J Geophys Res Oceans 123:7511–7528

Krupica KL, Sprules WG, Herman AW (2012) The utility of body size indices derived from optical plankton counter data for the characterization of marine zooplankton assemblages. Cont Shelf Res 36:29–40

Kwong LE, Henschke N, Pakhomov EA, Everett JD, Suthers IM (2020) Mesozooplankton and micronekton active carbon transport in contrasting eddies. Front Mar Sci 6:825

Lee TN, Yoder JA, Atkinson LP (1991) Gulf Stream frontal eddy influence on productivity of the southeast US continental shelf. J Geophys Res Oceans 96:22191–22205

Leis JM, Carson-Ewart BM (2000) The larvae of Indo-Pacific coastal fishes: an identification guide to marine fish larvae. Brill, Leiden

Lenth R (2018) Emmeans: estimated marginal means, aka least-squares means. https://cran.r-project.org/web/packages/emmeans/index.html

Logerwell EA, Smith PE (2001) Mesoscale eddies and survival of late stage Pacific sardine (*Sardinops sagax*) larvae. Fish Oceanogr 10:13–25

Malan N, Archer M, Roughan M, Cetina-Heredia P and others (2020) Eddy-driven cross-shelf transport in the East Australian Current separation zone. J Geophys Res Oceans 125:e2019JC015613

Matis PA, Figueira WF, Suthers IM, Humphries J and others (2014) Cyclonic entrainment? The ichthyoplankton attrib-

utes of three major water mass types generated by the separation of the East Australian Current. ICES J Mar Sci 71:1696–1705

Moyano M, Rodríguez JM, Benítez-Barrios VM, Hernández-León S (2014) Larval fish distribution and retention in the Canary Current system during the weak upwelling season. Fish Oceanogr 23:191–209

Muhling BA, Beckley LE, Olivar MP (2007) Ichthyoplankton assemblage structure in two meso-scale Leeuwin Current eddies, eastern Indian Ocean. Deep Sea Res II 54: 1113–1128

Mullaney TJ, Suthers IM (2013) Entrainment and retention of the coastal larval fish assemblage by a short-lived, submesoscale, frontal eddy of the East Australian Current. Limnol Oceanogr 58:1546–1556

Mullaney TJ, Miskiewicz AG, Baird ME, Burns PTP, Suthers IM (2011) Entrainment of larval fish assemblages from the inner shelf into the East Australian Current and into the western Tasman Front. Fish Oceanogr 20:434–447

Mullaney TJ, Gillanders BM, Heagney EC, Suthers IM (2014) Entrainment and advection of larval sardine, *Sardinops sagax*, by the East Australian Current and retention in the western Tasman Front. Fish Oceanogr 23:554–567

Nakata H, Kimura S, Okazaki Y, Kasai A (2000) Implications of meso-scale eddies caused by frontal disturbances of the Kuroshio Current for anchovy recruitment. ICES J Mar Sci 57:143–152

Neira FJ, Miskiewicz AG, Trnski T (1998) Larvae of temperate Australian fishes: laboratory guide for larval fish identification. UWA Publishing, Perth, Nedands

Nieto K, McClatchie S, Weber ED, Lennert-Cody CE (2014) Effect of mesoscale eddies and streamers on sardine spawning habitat and recruitment success off Southern and central California. J Geophys Res Oceans 119: 6330–6339

Oke PR, Roughan M, Cetina-Heredia P, Pilo GS and others (2019) Revisiting the circulation of the East Australian Current: its path, separation, and eddy field. Prog Oceanogr 176:102139

Oksanen J, Blanchet FG, Friendly M, Kindt R and others (2018) Vegan: community ecology package. https://cran.r-project.org/web/packages/vegan/index.html

Olivar MP, Sabatés A, Pastor MV, Pelegrí JL (2016) Water masses and mesoscale control on latitudinal and cross-shelf variations in larval fish assemblages off NW Africa. Deep Sea Res I 117:120–137

Paxton JR, Hulley PA (1999) Families Neoscopelidae, Myctophidae. In: Carpenter KE, Niem VH (eds) The living marine resources of the Western Central Pacific, Vol 3. FAO Species Identification Guide for Fisheries Purposes. FAO, Rome, p 1955–1965

Paxton JR, Ahlstrom EH, Moser HG (1984) Myctophidae: relationships. In: Moser HG, Richards WJ, Cohen DM, Fahay MP, Kendall AW, Richardson SL (eds) Ontogeny and systematics of fishes. Special Publication. American Society for Ichthyology and Herpetology, Lawrence, KS, p 239–244

R Core Team (2017) R: a language and environment for statistical computing. R Foundation for Statistical Computing, Vienna. www.R-project.org/

Roughan M, Keating SR, Schaeffer A, Heredia PC and others (2017) A tale of two eddies: the biophysical characteristics of two contrasting cyclonic eddies in the East Australian Current System. J Geophys Res Oceans 122: 2494–2518

Schaeffer A, Gramoulle A, Roughan M, Mantovanelli A (2017) Characterizing frontal eddies along the East Australian Current from HF radar observations. J Geophys Res Oceans 122:3964–3980

Schilling HT, Everett JD, Smith JA, Stewart J and others (2020) Multiple spawning events promote increased larval dispersal of a predatory fish in a western boundary current. Fish Oceanogr 29:309–323

Schilling HT, Hinchliffe C, Gillson JP, Miskiewicz AG, Suthers IM (2022) Coastal winds and larval fish abundance indicate a recruitment mechanism for southeast Australian estuarine fisheries. Fish Oceanogr 31:40–55

Shulzitski K, Sponaugle S, Hauff M, Walter K, D'Alessandro EK, Cowen RK (2015) Close encounters with eddies: oceanographic features increase growth of larval reef fishes during their journey to the reef. Biol Lett 11: 20140746

Shulzitski K, Sponaugle S, Hauff M, Walter KD, Cowen RK (2016) Encounter with mesoscale eddies enhances survival to settlement in larval coral reef fishes. Proc Natl Acad Sci USA 113:6928–6933

Shulzitski K, Sponaugle S, Hauff M, Walter KD, D'Alessandro EK, Cowen RK (2018) Patterns in larval reef fish distributions and assemblages, with implications for local retention in mesoscale eddies. Can J Fish Aquat Sci 75: 180–192

Smith KA, Suthers IM (1999) Displacement of diverse ichthyoplankton assemblages by a coastal upwelling event on the Sydney shelf. Mar Ecol Prog Ser 176:49–62

Sponaugle S, Lee T, Kourafalou V, Pinkard D (2005) Florida Current frontal eddies and the settlement of coral reef fishes. Limnol Oceanogr 50:1033–1048

Suthers IM (2015) Submesoscale processes — billows and eddies — along the productive shelf by the East Australian Current. Voyage Report. https://mnf.csiro.au/en/Voyages/IN2015_V03

Suthers IM, Taggart CT, Rissik D, Baird ME (2006) Day and night ichthyoplankton assemblages and zooplankton biomass size spectrum in a deep ocean island wake. Mar Ecol Prog Ser 322:225–238

Suthers IM, White Z, Hinchliffe C, Falster DS, Richardson AJ, Everett JD (2021) The Mortality/Growth ratio of larval fish and the slope of the zooplankton size-spectrum. Fish Fish (in press) doi:10.1111/faf.12633

Syahailatua A, Roughan M, Suthers IM (2011) Characteristic ichthyoplankton taxa in the separation zone of the East Australian Current: larval assemblages as tracers of coastal mixing. Deep Sea Res II 58:678–690

Tiedemann M, Fock HO, Döring J, Badji LB, Möllmann C (2018) Water masses and oceanic eddy regulation of larval fish assemblages along the Cape Verde Frontal Zone. J Mar Syst 183:42–55

Waite AM, Muhling BA, Holl CM, Beckley LE and others (2007) Food web structure in two counter-rotating eddies based on $\delta^{15}N$ and $\delta^{13}C$ isotopic analyses. Deep Sea Res II 54:1055–1075

Wang Y, Naumann U, Wright ST, Warton DI (2012) Mvabund — an R package for model-based analysis of multivariate abundance data. Methods Ecol Evol 3: 471–474

Warton DI, Wright ST, Wang Y (2012) Distance-based multivariate analyses confound location and dispersion effects. Methods Ecol Evol 3:89–101

Appendix. Full list of author addresses

Valquiria Garcia[1,2], Hayden T. Schilling[1,3], Derrick O. Cruz[1], Steven M. Hawes[4], Jason D. Everett[1,3,5], Moninya Roughan[6], Anthony G. Miskiewicz[1,7], Evgeny A. Pakhomov[8,9], Andrew Jeffs[10], Iain M. Suthers[1,3]

[1]School of Biological, Earth & Environmental Sciences, University of New South Wales, Sydney, NSW 2052, Australia

[2]Laboratório de Biologia e Cultivo de Peixes de Água Doce, Universidade Federal de Santa Catarina, Florianópolis 88066-260, Brazil

[3]Sydney Institute of Marine Science, Mosman, NSW 2088, Australia

[4]School of Life and Environmental Sciences, University of Sydney, Sydney, NSW 2006, Australia

[5]Centre for Applications in Natural Resource Mathematics, School of Mathematics and Physics, The University of Queensland, St Lucia, QLD 4072, Australia

[6]School of Mathematics and Statistics, UNSW Sydney, NSW 2052, Australia

[7]Ichthyology Department, Australian Museum Research Institute, Australian Museum, Sydney, NSW 2010, Australia

[8]Department of Earth, Ocean and Atmospheric Sciences, and Institute for the Oceans and Fisheries, University of British Columbia, Vancouver, BC V6T 1Z4, Canada

[9]Hakai Institute, Heriot Bay, BC V0P 1H0, Canada

[10]School of Biological Sciences and Institute of Marine Science, University of Auckland, Private Bag 92019, Auckland 1142, New Zealand

Editorial responsibility: Alejandro Gallego, Aberdeen, UK
Reviewed by: M. Tiedemann and 2 anonymous referees

Submitted: August 17, 2021
Accepted: December 14, 2021
Proofs received from author(s): February 23, 2022